Relationship between the Temperatures of Solar Corona and Planetary Magnetosheaths

Chao Shen[1], Nian Ren[1], Yonghui Ma[1], **M. N. S. Qureshi[2], and Yang Guo[3]**

[1]School of Science, Harbin Institute of Technology, Shenzhen, 518055, China.

[2]Department of Physics, GC University, Lahore 54000, Pakistan.

[3]School of Astronomy and Space Science and Key Laboratory for Modern Astronomy and Astrophysics, Nanjing University, Nanjing 210023, China

Corresponding author: Chao Shen (shenchao@hit.edu.cn)

Key Points:

1. Quantitative relationship between the temperatures of the steady solar corona and planetary magnetosheaths has been yielded
2. All the planetary magnetosheaths have comparable maximum temperatures, which are equal to or lower than that of the corona
3. The statistical investigation confirms the theoretical results

Abstract

This research aims to explore the relationship between the temperatures of solar corona and planetary magnetosheaths. Based on the second law of thermodynamics, the maximum temperatures of the planetary magnetosheaths cannot be higher than that of the solar corona. A theoretical investigation has been made on the expansion of solar corona, the propagation of solar wind and the compressions of planetary magnetosheaths by the bow shocks. The method used is general and fit for the dynamics of multiple components, thermal anisotropy, and non-Maxwellian plasmas in a steady state, and approximate formulas have been obtained. It is found that, for the steady situations, the temperatures of all the planetary magnetosheaths at the subsolar points in the solar system have comparable values, which are also close to the maximum temperature of the solar corona. Secondly, a systematic statistical survey on the average temperatures of the planetary magnetosheaths have been carried out, which show that, the average plasma temperatures of the magnetosheaths of Earth and Saturn are 183eV (2.12MK) and 172eV (2.00MK), respectively. The statistical results are consistant with the theoretical results. These results are very practical for the estimations of the thermal properties of the planetary magnetospheres.

Key Words

Solar Corona, Solar Wind, Bow Shocks, Planets, Magnetosheaths, Temperatures

Plain Language Summary

This research has made stress on the relationship between the temperatures of the planetary magnetosheaths and solar corona, which is an interdisciplinary problem in the solar–terrestrial physics. A theoretical investigation has been made on the expansion of solar corona, the propagation of solar wind and the compressions of planetary magnetosheath by the bow shocks. The approximate formula for the relationship between the temperatures of the solar corona and planetary magnetosheaths has been obtained. The quantitative results indicate that, the maximum temperatures of the planetary magnetosheaths have comparable values, which are generally close to that of the solar corona. A statistical investigation on the average temperatures of the magnetosheaths of several planets have been made, and it is shown that, although the proton temperatures are several times of the electron temperatures, the average plasma temperatures of the magnetosheaths of Earth and Saturn are almost the same as that of the solar corona. This work will make advancement in our understanding on the thermal properties of the planetary magnetosheaths and also benefit the research on the formation of the plasma sheets.

1 Introduction

Magnetosheaths are important sources of plasmas in the planetary magnetospheres, partially control the thermal state of the magnetospheric plasmas, and play critical role in the dynamical evolution of the planetary magnetospheres (Chapman et al., 1930; Axford et al., 1961; Dungey, 1961; Song et al., 1990, 1992, 1994, 1999a,b; Southwood and Kivelson,1995, 2020; Phan et al., 2000; Fujimoto et al., 2008; Taylor et al., 2008; Wang et al., 2012). The solar wind, which originates from the solar corona, interacts with the intrinsic magnetic field of the planets and shapes the magnetospheres. Upon impacting the magnetospheres, the supersonic solar wind will form bow shocks, which surround the magnetospheres with conicoid surface shapes (Shue et al., 1998; Dmitriev et al., 2003; Chao et al., 2002; Shen et al., 2007; Shen et al., 2020). The upstream solar wind is compressed by the bow shocks so as to form the downstream magnetosheath plasmas between the bow shocks and the magnetopauses. The density and temperature of the magnetosheath plasmas maximums at the stagnation point and are decreasing gradually downstream (Spreite and Alksne, 1969; Song et al., 1990, 1999a; Southwood and Kivelson, 2020). Therefore, the thermal properties of the magnetosheath plasmas should be controlled by the features of the solar corona.

The corona is extremely hot with a temperature of millions of Kelvin, that is much higher than that of the photosphere of Sun (～5770K). The heating mechanism is not clear and still under investigations (McComas et al., 2007; Parnell et al., 2012; Klimchuk, 2015; Cranmer et al., 2017). Observations have shown that, the quiet corona has a temperature of 0.5-3 Million K (MK), here it is noted that 1MK≈86.17eV (Laming et al., 1995; Delaboudinière et al., 1995). In the solar active regions, the temperature of the corona can reach up to ～3-5MK (350-580eV) (Delaboudinière et al., 1995; Schrijveret et al., 1999; Schmelz et al., 2015). The temperature of the ions in the coronal holes can be as high as 2.5-5.0MK (300-580eV) (Tu et al., 1999).

The extremely hot corona expands outward and generates outflowing solar wind into the interplanetary space (Parker, 1958; Barnes, 1992; Marsch, 1999; Cranmer et al., 2017). In the space near the Sun, the solar wind is accelerated rapidly (McComas et al., 2007). With the increasing distance from the Sun, the velocity of the solar wind becomes larger and larger, while its density and temperature decrease gradually (Parker, 1958; Barnes et al., 1992; Marsch, 1999; Koet et al.,1999; McComas et al., 2007, 2008; Cranmeret et al.,2017). As indicated by Parker's model (Parker, 1958), the velocity of the solar wind far away from the Sun varies with the heliocentric distance r and approximately follows the formula $V = 2V_c \left(\ln(r / r_c)\right)^{1/2}$, where r_c is Parker critical heliocentric distance and V_c is the critical velocity, while the density of the solar wind is $n \propto (Vr^2)^{-1}$ according to the conservation of matter. The temperature of the solar wind is dropping with the distance from the Sun as

105 $\mathrm{T} \propto r^{-\alpha}$, where the factor α ranges from 2/7 to 4/3 (Barnes, 1992; McComaset et al.,
106 2008; Cranmer et al., 2009; Scudder, 2015). Weber and Davis (1967) has established a
107 steady solar wind model with considering the azimuthal motion of the solar wind,
108 which indicated that the magnetic field in the solar wind may apply a torque to the
109 Sun and lead to the loss of the angular momentum of the Sun. As the solar wind
110 reaches at the location of Earth with a heliocentric distance of 1AU, actual
111 measurements reveal that (Burlaga and Szabo, 1999), its mean velocity is
112 $\overline{\mathrm{V}} \approx 400\mathrm{km}\cdot\mathrm{s}^{-1}$, mean density is $\bar{n} \approx 5\mathrm{cm}^{-3}$, while its average electron temperature
113 $\mathrm{T}^e \approx 0.1-0.2\mathrm{MK}$ (12-25eV), and average proton temperature
114 $\mathrm{T}^p \approx 0.01-0.4\mathrm{MK}$ (1.2-50eV), with average plasma temperature being
115 $\langle T \rangle_{sw} \approx \frac{1}{2}(T^e + T^p) \approx 0.13\mathrm{MK}$ (15eV), if Helium ions are omitted (Burlaga and Szabo,
116 1999; Cranmer et al., 2017).

117 On the other hand, the solar wind is expanding with the magnetic field frozen
118 in. According to the Parker spiral field model, the radial component of the
119 interplanetary magnetic field (IMF) is $B_r \propto 1/r^2$, while its azimuthal component is
120 $B_\phi \propto (r-r_0)/r^2$ (Parker, 1958). In the vicinity of Earth at 1AU, the magnetic strength
121 of the IMF is ~6nT with the IMF spiral angle being $\sim 45^\circ$, and the ratio between the
122 thermal energy and magnetic energy in the solar wind is $\beta \sim 0.1\text{-}6$ (Burlaga and
123 Szabo, 1999).

124 If the expansion of corona and solar wind can be regarded as a heat engine
125 process, its thermal efficiency at 1AU is $\zeta = (T_{cor} - \langle T \rangle_{sw})/T_{cor} \approx 1 - 1.3\times10^5/(3\times10^6) = 96\%$.
126 So, the solar corona heat engine is rather effective in respect of transferring heat into

kinetic energy. When the solar wind passes by the planets, such as Mercury, Earth, Jupiter, Saturn, etc., it impacts the magnetic field of the planets so as to produce the planetary magnetospheres and bow shocks. The upstream solar wind traverses the bow shocks and will be compressed to form the denser and hotter plasmas of the magnetosheaths (Petrinec and Russell, 1997; Chapman et al., 2004; Masters et al., 2011). The physical parameters of the upstream solar wind and the downstream magnetosheath plasmas approximately obey Rankine-Hugoniot jump conditions (Hudson, 1970; Liu et al., 2007). The observations by the Mercury Surface, Space Environment, Geochemistry, and Ranging (MESSENGER) show that, the proton temperature in Mercury magnetosheath at the subsolar point is $T^p \approx 1.2-8.4\mathrm{MK}$ (150-980eV) with the most probable proton temperature being $T_{mp}^p \approx 3\mathrm{MK}\,(350\mathrm{eV})$ (Gershman et al., 2013). Under extreme solar wind conditions, the proton temperature in Mercury magnetosheath can be up to 6.0 MK (700eV) (Slavinet et al., 2014). According to the observations by the Double Star Project (DSP) during the year 2004-2005 (Liu et al., 2005; Shen et al., 2005) the time averaging electron temperature of Earth's magnetosheath at the dayside is $T^e \approx 50eV$, while the time averaging ion temperature is $T^i \approx 200eV$ (Shen et al., 2008). Therefore, the average plasma temperature in Earth's magnetosheath at the dayside is about $\langle T \rangle_{sh} \approx \frac{1}{2}\left(T^e + T^i\right) \approx 125eV$. The statistical analysis on the THEMIS observations (Wang et al., 2012) indicates that, at the subsolar point of the Earth's dayside magnetosheath, the mean electron and ion temperatures are $T^e \approx 40eV$ and $T^i \approx 210eV$, respectively; thus the average plasma temperature at the subsolar point of

149 the Earth's magnetosheath is $\langle T \rangle_{sh} \approx \frac{1}{2}\left(T^e + T^i\right) \approx 125eV$. For fast solar wind
150 conditions, the mean electron and ion temperatures at the subsolar point of the Earth's
151 magnetosheath are $T^e \approx 53eV$ and $T^i \approx 400eV$, respectively, with the average plasma
152 temperature being $\langle T \rangle_{sh} = \frac{1}{2}\left(T^e + T^i\right) \approx 227eV$. Based on the measurements by
153 Voyager 1 & 2 on the Jupiter and Saturn, Richardson (1987, 2002) have revealed that
154 the protons in the magnetosheath of Jupiter and Saturn have a double-Maxwellian
155 distribution, and are composed of both cold and hot components with temperatures
156 $T_C^p \approx 100eV$ and $T_H^p \approx 600eV$, respectively. These two components of protons have
157 comparable densities, therefore the average proton temperature of the magnetosheath
158 of Jupiter and Saturn is estimated as $T^p \approx (T_C^p + T_H^p)/2 \approx 350eV$. The explorations of
159 Cassini on Saturn have shown that the average ion temperature of the Saturn's
160 magnetosheath is $T^i \approx 210 - 370eV$ (Sergiset et al., 2013). Thomsen et al. (2018)
161 made a detailed survey on the features of Saturn's magnetosheath based on Cassini
162 measurements and showed that the mean temperatures of the electrons and protons at
163 the subsolar point of Saturn's magnetosheath are $T^e \approx 34eV$ and $T^p \approx 340eV$,
164 respectively, with the average temperature of the Saturn's magnetosheath being
165 $\langle T \rangle_{sh} = \frac{1}{2}\left(T^e + T^i\right) \approx 187eV$. Both the temperatures of electrons and protons from the
166 Saturn's magnetosheath are gradually decreasing as we move away from the noon
167 (Thomsen et al., 2018). Therefore, the observations indicate that, the plasma
168 temperatures of the planetary magnetosheaths have comparable values of about
169 several MK or several hundred eV, which are very near to that of solar corona.

170 Satellite observations of velocity distribution functions (VDFs) from solar

wind and the magnetosheaths of planets (such as Earth, Mercury, Saturn and Uranus) frequently show non-Maxwellian features. Such distributions exhibit suprathermal tails at high energies and quasi-Maxwellian behavior at low energies [Christon et al., 1988; Maksimovic et al., 1997; Pierrard et al., 2004]. Non-Maxwellian VDFs have also been found in the solar wind and around Earth's bow shock with two different temperatures and densities, with 'core' a dense thermal population superimposed on 'halo' a superthermal hot population [Feldman et al. 1975; 1983a; 1983b; Lin 1998; March 2006; Gaelzer et al., 2008]. Distributions superthermal tails are well modelled by kappa distribution since it fits both the Maxwellian (thermal) and non-Maxwellian (superthermal) high energy part of the distribution [Pierrard and Lemaire, 1996; Schippers et al. 2008]. Electron VDFs in the Earth's magnetosheath and magnetosphere have also been observed with flat tops instead of quasi-Maxwellian low energy part, which could not be fitted either by Maxwellian or kappa distribution functions. Such observed flat top VDFs often showed one and two distinct components and are well fitted by generalized (r,q) distribution function [Qureshi et al., 2004; 2019; Sumbul et al., 2019]. It is known that the magnetosheaths are also rather turbulent and filled with various waves, such as the fast and slow magnetosonic waves, the Alfven eaves, and mirror modes, whistler waves, even solitary waves (Sckopke, et al., 1990; Song et al., 1990, 1992, 1994; Southwood and Kivelson,1995).

As for the simplified cases when the magnetic field, solar gravity, and coronal heat conduction could be omitted, the expansion of the solar corona could be regarded as an adiabatic process, with the plasma entropy conserved. The coronal plasmas with

193 an extremely high temperature expand outward from a stationary state, accelerated in
194 the interplanetary space, and decelerated by the bow shocks in the vicinity of planets
195 so as to form the hot magnetosheath plasmas with very small bulk velocities.
196 According to the second law of thermodynamics, the plasma temperatures of the
197 planetary magnetosheaths cannot be larger than the maximum temperature of the
198 source region plasmas—the solar corona, i.e. $T_{sh} \le T_{cor}$. However, in the actual
199 situations, a part of the thermal energy of the corona will be spent to overcome the
200 pull of the solar gravity, and the magnetic field in the corona may also accelerate the
201 solar wind. Furthermore, the electrons and ions of the solar wind or the
202 magnetosheaths have different temperatures. So that, it is one complicated problem
203 associated with many factors. Therefore, it is necessary to have a detailed theoretical
204 investigation on the whole process of the outward expansion of the solar corona,
205 propagation of the solar wind and the compression of the planetary magnetosheaths
206 by the bow shocks, so as to find the quantitative relationship between the
207 temperatures of the solar corona and the planetary magnetosheaths.

208 In this research, a theoretical analysis on the motion of the solar wind has been
209 made in Section 2 and approximate formulas relating the maximum temperatures of
210 solar corona and the planetary magnetosheaths for the steady situations presented;
211 statistical investigations on the features of the plasma temperatures in planetary
212 magnetosheaths have been carried out in Section 3; at last discussion and conclusions
213 are given in Section 4.

214

2 Theoretical Analysis on the Physical Processes

Here the propagation of the multiple components, thermal anisotropy and non-Maxwellian solar wind from the corona to the planetary magnetosheaths have been investigated. It has been shown that multi-component magnetohydrodynamic (MHD) is effective for approximately describing the coronal expansion and the propagation of the solar wind (Parker, 1958; Echim et al., 2011).

In the solar system, the planets are orbiting the Sun about at the ecliptic plane. We may investigate the steady propagation of the solar wind at the ecliptic plane, which is illustrated in Figure 1. To make the physics explicit and facilitate the analysis, we first present a short derivation of the Bernoulli's equation applicable for the multiple components, thermal anisotropy and non-Maxwellian solar wind.

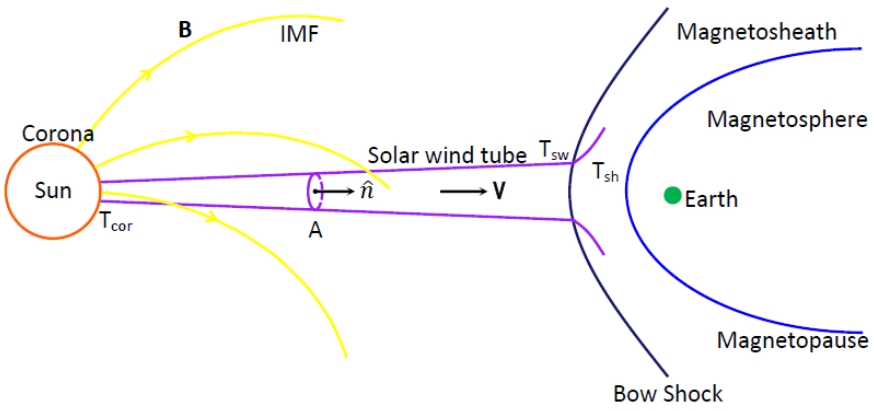

Figure 1. Propagation of the solar wind from the corona to the Earth's magnetosheath

The steady coronal solar wind and magnetosheath plasmas obey the equation of continuity

$$\frac{\partial \rho}{\partial t} = -\nabla \cdot (\rho \mathbf{V}) = 0, \tag{1}$$

where， $\mathbf{V}$ and ρ are the bulk velocity and mass density of the plasmas, respectively. For simplicity, it is assumed that the electrons and ions of plasmas have the same bulk velocities. Generally, it is proper to denote $\mathbf{V} = V\hat{\mathbf{n}}$， here $\hat{\mathbf{n}}$ is the unit radial vector with respect to the heliocenter. The mass density of the plasmas can be expressed as $\rho=\sum_{a} n_a m_a$, here m_a and n_a are the mass and number density of the species a, respectively.

The steady expansion of the corona, propagation of the solar wind and compression of the magnetosheath plasmas also obey the following equation of energy (Rossi et al., 1970; Echim et al., 2011)

$$\frac{\partial}{\partial t}\left(\frac{1}{2}\rho V^2+\varepsilon_T+\varepsilon_{em}+\rho\phi\right)=-\nabla\cdot\left[\mathbf{P}\cdot\mathbf{V}+\left(\frac{1}{2}\rho V^2+\varepsilon_T\right)\mathbf{V}+\mathbf{S}_{em}+\left(\rho\phi\right)\mathbf{V}+\boldsymbol{q}\right]=0\text{，}\quad(2)$$

where the total energy of the solar wind is composed of the kinetic, thermal, electromagnetic and gravitational potential. The thermal energy density of the solar wind is

$$\varepsilon_T=\sum_a \varepsilon_T^a=\sum_a n_a\left(\frac{1}{2}kT_{\parallel}^a+kT_{\perp}^a\right).\quad(3)$$

Here, ε_T^a is the thermal energy density of the species a, $T_{\parallel}^a$ and $T_{\perp}^a$ are the temperatures of the species ‘a’ parallel and perpendicular to the magnetic field, respectively, k is the Boltzmann constant and ε_{em} is the electromagnetic energy density. The gravitational potential is $\phi=-GM_S/r$，where G is the gravitational constant, M_S is the mass of the Sun, r is the heliocentric distance. In contrast with the solar gravity, those of the planets are rather weak and their effects on the solar wind can be omitted. The thermal pressure tensor of the species a is defined as

$P_{ij}^{a} = \int v_i p_j f_a(\mathbf{x},\mathbf{p}) d^3\mathbf{p}$, in the frame of reference of the plasma bulk velocity $\mathbf{V}$, where $f_a(\mathbf{x},\mathbf{p})$ is the phase space density of the species a in the space of positions $\mathbf{x}$ and momentum $\mathbf{p}$ (Rossi et al., 1970). The phase space densities of the solar wind and planetary magnetosheath plasmas can be non-Maxwellian (Vasyliunaus et al., 1968; Maksimovic et al., 1997; Masood et al., 2006; Richardson, 2002; Qureshi et al., 2014; Qureshi et al., 2019a, b). The components of the total thermal pressure tensor $\mathbf{P}$ of the magnetized plasmas in the coordinates of the magnetic field is

$$P_{ij} = \sum_a P_{ij}^{a} = \sum_a \begin{pmatrix} P_{\perp}^{a} & 0 & 0 \\ 0 & P_{\perp}^{a} & 0 \\ 0 & 0 & P_{\parallel}^{a} \end{pmatrix}, \quad (4)$$

where the pressures of the species a parallel and perpendicular to the magnetic field are $P_{\perp}^{a} = n_a k T_{\perp}^{a}$ and $P_{\parallel}^{a} = n_a k T_{\parallel}^{a}$, respectively. The flux density of electromagnetic energy is

$$\mathbf{S}_{em} = \frac{\mathbf{E}\times\mathbf{B}}{\mu_0}. \quad (5)$$

Generally, the magnetic flux is frozen in the plasmas and $\mathbf{E} = -\mathbf{V}\times\mathbf{B}$, so that $\mathbf{S}_{em} = \frac{\mathbf{1}}{\mu_0}(\mathbf{B}\times\mathbf{V})\times\mathbf{B} = \frac{1}{\mu_0}\left[B^2\mathbf{V} - (\mathbf{B}\cdot\mathbf{V})\mathbf{B}\right]$. In Eq. (2), $\mathbf{q}$ is the total heat flux in the solar wind. Presently, we still do not understand the heating mechanism of the solar corona and it is a problem still under investigation (McComas et al., 2007; Parnell et al., 2012; Klimchuk, 2015; Cranmeret et al.,2017). As indicated by the observations that the heating and radiative losses are at an equilibrium in the core region of the solar corona, so as to maintain the extremely high temperature of the coronal plasmas. This investigation has been carried out under the assumption that the coronal plasmas

expand under the thermodynamic force or pressure so as to produce the solar wind flowing outward. Therefore the heating and radiative loss in the coronal region will not be considered here.

Applying the equation of conservation of energy (2) in the steady situation to the solar wind tube with cross-sectional area A as indicated in Figure 1, yields

$$A\hat{\mathbf{n}}\cdot\left[\mathbf{P}\cdot\mathbf{V}+\left(\frac{1}{2}\rho V^2+\varepsilon_T\right)\mathbf{V}+\mathbf{S}_{em}+(\rho\phi)\mathbf{V}+\boldsymbol{q}\right]=\text{Const}, \tag{6}$$

or

$$\left[P_{nn}V+\left(\frac{1}{2}\rho V^2+\varepsilon_T\right)V+\frac{1}{\mu_0}B_t^2V-\rho\frac{GM_S}{r}V+q_n\right]A=\text{Const}, \tag{6'}$$

where $P_{nn}=\hat{\mathbf{n}}\bullet P\bullet\hat{\mathbf{n}}$ and $\mathbf{S}\bullet\hat{\mathbf{n}}=\frac{1}{\mu_0}\left[(\mathbf{B}\times\mathbf{V})\times\mathbf{B}\right]\cdot\mathbf{n}=\frac{1}{\mu_0}(\mathbf{B}\times\hat{\mathbf{n}})\cdot(\mathbf{B}\times\mathbf{V})=\frac{|\mathbf{B}\times\hat{\mathbf{n}}|^2}{\mu_0}V$ $=\frac{1}{\mu_0}B_t^2V$. Here B_t is the component of magnetic field in the direction perpendicular to the radial direction.

On the other hand, the continuity equation (1) reduces to

$$\rho V\cdot A=\text{Const}. \tag{7}$$

Comparing the equations (6') and (7) yields

$$\left(\frac{P_{nn}}{\rho}+\frac{1}{2}V^2+\frac{\varepsilon_T}{\rho}+\frac{B_t^2}{\mu_0\rho}-\frac{GM_S}{r}+\frac{q_n}{\rho V}\right)=\text{Const}. \tag{8}$$

Equation (8) is the Bernoulli's equation for multiple components, thermal anisotropic and non-Maxwellian solar wind plasmas. It is noted that, only the laws of conservation of matter and energy (equations (1) and (2)) have been used in the above deducing, but the momentum conservation equation has not applied. So that the

equation (8) obtained above is not a complete description of the dynamical evolution of the corona, solar wind and magnetoshesths. The formula (8) relates the thermal properties of the corona, solar wind and planetary magnetoshesths, but is not able to provide the definite features of their motions. Their velocities can be given the observations directly.

Denote the angle between $\mathbf{V}$ and $\mathbf{B}$ as θ. In the steady situation, $\theta \approx 0^{\circ}$ in the outer corona, while $\theta \approx 45^{\circ}$ at 1AU. In the Cartesian coordinates with respect of the magnetic field as illustrated in Figure 2,

$\hat{\mathbf{n}} = \cos\theta \hat{\mathbf{e}}_z + \sin\theta \hat{\mathbf{e}}_x$, $\mathbf{P} = P_{\parallel}\hat{\mathbf{e}}_z\hat{\mathbf{e}}_z + P_{\perp}\left(\hat{\mathbf{e}}_x\hat{\mathbf{e}}_x + \hat{\mathbf{e}}_y\hat{\mathbf{e}}_y\right)$, therefore

$$P_{nn} = \hat{\mathbf{n}}\cdot\mathbf{P}\cdot\hat{\mathbf{n}} = \cos^2\theta P_{\parallel} + \sin^2\theta P_{\perp} = \sum_a \left(\cos^2\theta n_a kT_{\parallel}^a + \sin^2\theta n_a kT_{\perp}^a\right) \quad (9)$$

.

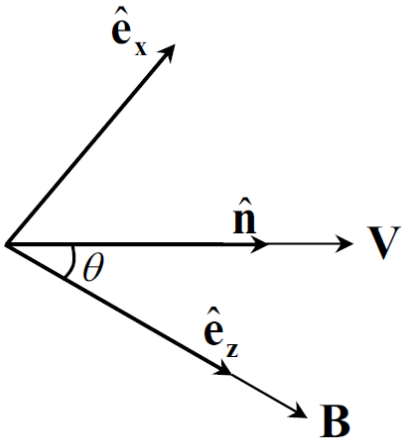

Figure 2. Demonstration of the Cartesian coordinates with respect of the magnetic field. It is chosen that, the z axis is along the direction of magnetic field B, and the radial direction $\hat{\mathbf{n}}$ is at the x-z coordinate plane.

Here the transverse plasma beta is defined as $\beta_t = \varepsilon_T / \left(\frac{B_t^2}{2\mu_0}\right)$, that is the ratio between the total thermal energy ε_T and the transverse magnetic field energy

$B_t^2/2\mu_0$. So the Bernoulli's equation (8) becomes

$$\frac{1}{2}V^2+\frac{1}{\rho}\left(P_{nn}+\varepsilon_T+\frac{2}{\beta_t}\varepsilon_T\right)-\frac{GM_S}{r}+\frac{q_n}{\rho V}=\text{Const} \quad (10)$$

In the above equation, the term $\frac{GM_S}{r}=\frac{R_S}{r}\frac{GM_S}{R_S}=\left(\frac{R_S}{r}\right)V_E^2$, where $\frac{GM_S}{R_S}=V_E^2$, and the escape velocity $V_E\approx 438\text{km/s}$. Here, the gravitational constant $G\approx 6.67\times10^{-11}\text{m}^2/\left(\text{s}^2\cdot\text{kg}\right)$, the radius of the Sun $R_S\approx 6.69\times10^8\text{m}$, and the solar mass $M_S\approx 1.99\times10^{30}\text{kg}$. Then the Bernoulli's equation (10) can be written as

$$\frac{1}{2}V^2+\frac{1}{\rho}\left[P_{nn}+\left(1+2\beta_t^{-1}\right)\varepsilon_T\right]-\frac{R_S}{r}V_E^2+\frac{q_n}{\rho V}=\text{Const} \quad (11)$$

Commonly, the ion ratio He^{2+}/H^+ in the solar wind is less than 6% and around 4.5% on average (Song et al., 1999b; McComas et al., 2008; Cranmeret et al., 2017). In the solar wind plasmas, heavy elements are very rare, so we can just consider electrons, protons and $^4He^{2+}$ (or α particles) and neglect other ions, which is a reasonable approximation. Assume the ion ratio He^{2+}/H^+ in the solar wind be $\eta<0.06$, and the number densities of the protons, ions He^{2+} and electrons are n_p, $n_\alpha=\eta n_p$, and $n_e=n_p+2n_\alpha=(1+2\eta)n_p$, respectively. Then the total number density of the plasmas is $n=n_e+n_p+n_\alpha=(1+2\eta)n_p+n_p+\eta n_p=(2+3\eta)n_p$, and the mass density of the solar wind is

$$\rho=n_pm_p+\eta n_pm_\alpha+(1+2\eta)n_pm_e=n\mu m_p, \quad (12)$$

where m_e, m_p and m_α are the masses of the electrons, protons and He^{2+} ions. Considering $m_e\ll m_p$ and $m_\alpha\approx 4m_p$, the average atomic weight of the solar plasmas is $\mu\approx(1+4\eta)/(2+3\eta)$. Therefore, from Eq. (9) it yields

$$\frac{P_{nn}}{\rho}=\frac{k}{(\mathbf{2}+\mathbf{3}\eta)\mu m_p}\left\{\cos^2\theta\left[(1+2\eta)T_{\|}^{e}+T_{\|}^{p}+\eta T_{\|}^{\alpha}\right]+\sin^2\theta\left[(1+2\eta)T_{\perp}^{e}+T_{\perp}^{p}+\eta T_{\perp}^{\alpha}\right]\right\} \tag{13}$$

or

$$\frac{P_{nn}}{\rho}=\frac{k}{(2+3\eta)\mu m_p}\left[(1+2\eta)T_{n}^{e}+T_{n}^{p}+\eta T_{n}^{\alpha}\right], \tag{14}$$

here, the radial temperatures of the species 'a' (e, p, or α) are defined as

$$T_{n}^{a}=\cos^2\theta T_{\|}^{a}+\sin^2\theta T_{\perp}^{a}. \tag{15}$$

The total thermal energy density is

$$\varepsilon_T=\sum_a \varepsilon_a^T=\sum_a n_a\left(\frac{1}{2}kT_{\|}^{a}+kT_{\perp}^{a}\right). \tag{16}$$

The omnidirectional temperature of a species can be defined as

$$\frac{3}{2}k\bar{T}^{a}\equiv\frac{1}{2}kT_{\|}^{a}+kT_{\perp}^{a}. \tag{17}$$

Then the total thermal energy density in Eq. (16) becomes

$$\varepsilon_T=\frac{3}{2}nk\left[(1+2\eta)\bar{T}^{e}+\bar{T}^{p}+\eta\bar{T}^{\alpha}\right]/(2+3\eta). \tag{18}$$

We can regard that the average temperature of the plasmas is

$$\langle T\rangle\equiv\left[(1+2\eta)\bar{T}^{e}+\bar{T}^{p}+\eta\bar{T}^{\alpha}\right]/(2+3\eta). \tag{19}$$

For the situations when the Helium abundance is very small, the contribution of the He^{2+} ions can be neglected and the average temperature of the plasmas is $\langle T\rangle=(\bar{T}^{e}+\bar{T}^{p})/2$. Therefore, the Bernoulli's equation (11) reduces to

$$\frac{1}{2}V^2+\frac{k}{\mu m_p}\left[\frac{(1+2\eta)T_{n}^{e}+T_{n}^{p}+\eta T_{n}^{\alpha}}{2+3\eta}+\frac{3}{2}\left(1+2\beta_t^{-1}\right)\langle T\rangle\right]-\frac{R_S}{r}V_E^2+\frac{q_n}{\rho V}=\text{Const}. \tag{20}$$

Relating the corona to the planetary magnetosheaths, it yields

$$\frac{1}{2}V_{cor}^2+\frac{k}{\mu m_p}\left[\frac{(1+2\eta)T_n^e+T_n^p+\eta T_n^\alpha}{2+3\eta}+\frac{3}{2}\left(1+2\beta_t^{-1}\right)\langle T\rangle\right]_{cor}-\frac{R_S}{r_{cor}}V_E^2+\frac{q_n}{\rho V_{cor}}=$$

$$\frac{1}{2}V_{sh}^2+\frac{k}{\mu m_p}\left[\frac{(1+2\eta)T_n^e+T_n^p+\eta T_n^\alpha}{2+3\eta}+\frac{3}{2}\left(1+2\beta_t^{-1}\right)\langle T\rangle\right]_{sh}. \quad (21)$$

where the subscript "cor" and "sh" denote the corona and magnetosheaths, respectively. Here, the heat flux of the planetary magnetosheath collisionless plasmas has been neglected. At the subsolar point of the planetary magnetosheaths, the temperatures reach the maximum values, while the bulk velocities of the downstream plasmas are very small. According to the observational results of Wang et al., (2012) on Earth's magnetosheath and those of Thomsen et al., (2018) on Saturn's magnetosheath, in general, $V_{sh}\le 100\mathrm{km/s}$, $V_{sh}/V_{sw}\le 1/16$, $V_{sh}^2/V_{sw}^2\le 0.060$. As approaching the nose (the stagnant point) of the magnetopause along the Sun-planetary line, the velocity of the magnetosheath plasmas is decreasing to about zero. So the kinetic energy is much less than the total energy in the planetary magnetosheaths at the subsolar points and thus can be neglected. Similarly, the coronal velocity is very small and less than 100km/s in the corona region (Cranmer et al., 2017), therefore the first term at the left hand of Eq. (21) can also be neglected. Then the equation (21) is rewritten as

$$\frac{q_n}{\rho V}-\frac{R_S}{r_{cor}}V_E^2+\frac{k}{\mu m_p}\left[\frac{(1+2\eta)T_n^e+T_n^p+\eta T_n^\alpha}{2+3\eta}+\frac{3}{2}\left(1+2\beta_t^{-1}\right)\langle T\rangle\right]_{cor}=$$

$$\frac{k}{\mu m_p}\left[\frac{(1+2\eta)T_n^e+T_n^p+\eta T_n^\alpha}{2+3\eta}+\frac{3}{2}\left(1+2\beta_t^{-1}\right)\langle T\rangle\right]_{sh}. \quad (22)$$

For the steady corona, the magnetic field **B** is almost in the radial direction, i.e. $B_t\approx 0$, so the transverse plasma beta $\beta_t\gg 1$. Usually, all the species in the solar

corona are thermally isotropic, i.e. $T_n^a = \bar{T}^a$ (the transverse temperatures and the average temperatures are equal). So that, according to the definition (19), we can have in corona $\left((1+2\eta)T_n^e + T_n^p + \eta T_n^\alpha\right)/(2+3\eta) = \left((1+2\eta)\bar{T}^e + \bar{T}^p + \eta\bar{T}^\alpha\right)/(2+3\eta) = \langle T\rangle$. Furthermore, at the coronal region with the highest temperature T_{cor}^{max}, the gradient of the temperature is almost zero, i.e. $\nabla T_{cor} \approx 0$, so the heat flux can be neglected there. Therefore, equation (22) becomes

$$-\frac{R_S}{r_{cor}}\cdot\frac{\mu m_p V_E^2}{k} + \frac{5}{2}\cdot\langle T\rangle_{cor} = \left[\frac{(1+2\eta)T_n^e + T_n^p + \eta T_n^\alpha}{2+3\eta} + \frac{3}{2}\left(1+2\beta_t^{-1}\right)\langle T\rangle\right]_{sh}. \qquad (23)$$

The above formula shows the relationship between the maximum temperature of the solar corona and that of the planetary magnetosheaths at the subsolar points in the steady situation. It can be seen that, the maximum temperatures of the planetary magnetosheaths at the subsolar points are determined by the highest temperature of the solar corona. The transverse plasma beta β_t of the magnetosheaths at the right hand of the equation (23) is still not fixed because the equation of momentum has not been included in this investigation. The transverse plasma beta β_t of the magnetosheaths can be determined by the observations.

Now, we can consider the statistically averaged situations. For the electrons, protons and He^{2+} ions in the planetary magnetosheaths, their transverse temperatures are equal to their average temperatures, i.e., $T_n^e = \bar{T}^e$, $T_n^p = \bar{T}^p$, and $T_n^\alpha = \bar{T}^\alpha$ statistically. So that, with the definition (19), statistically the equation (23) becomes

$$-\frac{R_S}{r_{cor}}\cdot\frac{\mu m_p V_E^2}{k} + \frac{5}{2}\langle T\rangle_{cor} = \left(\frac{5}{2}+\frac{3}{\beta_t}\right)\langle T\rangle_{sh}. \qquad (24)$$

The above formula indicates that, the higher the plasma beta, the larger the values of

387 the temperatures of planetary magnetosheaths at the subsolar points.

388 Generally in the planetary magnetosheaths $\beta \sim 0.10\text{-}20$ (Richardson, 2002;

389 Gershman et al., 2013; Sergiset et al., 2013; Thomsen et al., 2018), and $\beta_t \geq \beta$. From

390 the above equation it is easy to obtain that

391 $$\langle \mathrm{T} \rangle_{\mathrm{cor}} \geq \langle \mathrm{T} \rangle_{\mathrm{sh}}, \tag{25}$$

392 or

393 $$\frac{1}{(2+3\eta)}\left((1+2\eta)\overline{\mathrm{T}}^{\mathrm{e}}_{\mathrm{cor}} + \overline{\mathrm{T}}^{\mathrm{p}}_{\mathrm{cor}} + \eta\overline{\mathrm{T}}^{\alpha}_{\mathrm{cor}}\right) \geq \frac{1}{(2+3\eta)}\left((1+2\eta)\overline{\mathrm{T}}^{\mathrm{e}}_{\mathrm{sh}} + \overline{\mathrm{T}}^{\mathrm{p}}_{\mathrm{sh}} + \eta\overline{\mathrm{T}}^{\alpha}_{\mathrm{sh}}\right). \tag{25'}$$

394 The above formula indicates that, the mean temperatures of the planetary

395 magnetosheaths are controlled by the mean temperature of the solar corona. In general,

396 the average temperatures of the planetary magnetosheaths at the subsolar points

397 cannot be higher than the maximum mean temperature of the solar corona. During the

398 expansion of the coronal plasmas, the gravity of the Sun acts to exhaust one part of

399 the thermal energy; on the other hand, during the compression of the magnetosheath

400 plasmas by the bow shocks, one part of the total energy is transferred into the

401 magnetic energy. So that, the average temperatures of the planetary magnetosheaths at

402 the subsolar points are lower than the maximum temperature of the solar corona, as

403 shown by the above equations (24)-(25). The statistical investigations have shown that,

404 the average temperature of Earth's magnetosheath at the subsolar point is

405 $\langle T \rangle_{sh} \approx 125eV$ or 1.45MK (Wang et al., 2012).

406 Usually, the planetary magnetosheaths (heliocentric distance is larger than 0.39AU)

407 may have a very high values of plasma beta. As an example, we may estimate the

mean value of plasma beta of Saturn's magnetosheath. As shown by the statistical investigations (Thomsen et al., 2018), the mean value of the proton beta of Saturn's magnetosheath at the subsolar point is $\beta_{\mathrm{p,sh}} \approx (\gamma-1)^{-1} \times 10 \approx 15$, where the factor $\gamma - 1 \approx 2/3$ arises from the difference of definitions on plasma beta. The proton-electron temperature ratio is much larger than 1 (Thomsen et al., 2018), and the electrons have much less contributions to the total thermal energy. So that the total plasma beta of the Saturn's magnetosheath at the subsolar point is $\beta_{\mathrm{sh}} \approx \beta_{\mathrm{p,sh}} \approx 15$ on average, and the corresponding mean transverse plasma beta is $\beta_{\mathrm{t,sh}} \approx 2\beta_{\mathrm{sh}} \approx 30 \gg 1$. During certain periods, there can be very weak magnetic field in the solar wind and magnetosheaths, $\beta_{\mathrm{t,sh}} \geq \beta_{\mathrm{sh}} \geq 1$. For these situations with $\beta \gg 1$, the formula (24) reduces to

$$-\frac{2}{5} \cdot \frac{\mathrm{R_S}}{\mathrm{r_{cor}}} \cdot \frac{\mu \mathrm{m_p} \mathrm{V_E^2}}{\mathrm{k}} + \langle \mathrm{T} \rangle_{\mathrm{cor}} \approx \langle \mathrm{T} \rangle_{\mathrm{sh}} . \tag{26}$$

The above formula implies that, for the cases when the planetary magnetosheaths have very high values of plasma beta, the planetary magnetosheaths has a mean temperature lower than the maximum temperature of corona. This result is surely consistent with the second law of thermodynamics if the plasma bulk velocity in the planetary magnetosheaths at the subsolar points is ignorable.

Therefore, in this research, we have verified that for the steady situations, the temperatures of all the planetary magnetosheaths at the subsolar points in the solar system have comparable values, which are less than the maximum one of the solar corona.

429 The above assumptions are correct for the steady cases and can be valid for the
430 average situations, but not applicable for the transient processes, such as the coronal
431 mass ejections (CMEs). Nevertheless, the theoretical results obtained above will be
432 supported by the statistical survey on the planetary magnetosheaths performed in the
433 next Section.

434

435 **3 Statistical Investigations**

436 We have had statistical investigations on the plasma temperatures in the
437 magnetosheaths of Mercury, Earth, Jupiter and Saturn, and made comparisons with
438 the theoretical results in the last section.

439 Figure 3 shows the distributions of ion temperatures in the magnetosheaths of
440 Mercury, Earth, Jupiter and Saturn, respectively. For Mercury, we use the data from
441 the Messenger satellite from 2012 to 2013. Based on the statistical analysis of the data
442 from 2012 to 2013, we can find that there are 94 days when the satellite is located in
443 Mercury's magnetosheath region. Based on the proton measurements during these
444 periods, we obtain the distribution of proton's temperatures in Mercury's
445 magnetosheath as shown in Figure 3. The temperatures of protons are drawn from the
446 NTP data in FIPS-DDR with the time resolution of 1 min. It can be seen from Figure
447 3 that the maximum proton temperature in Mercury's magnetosheath can reach up to
448 ~1500eV, with the most probable value of proton temperature being $T_{pm} \approx 275\text{eV}$,
449 and the average value $\overline{T_p} \approx 414\text{eV}$.

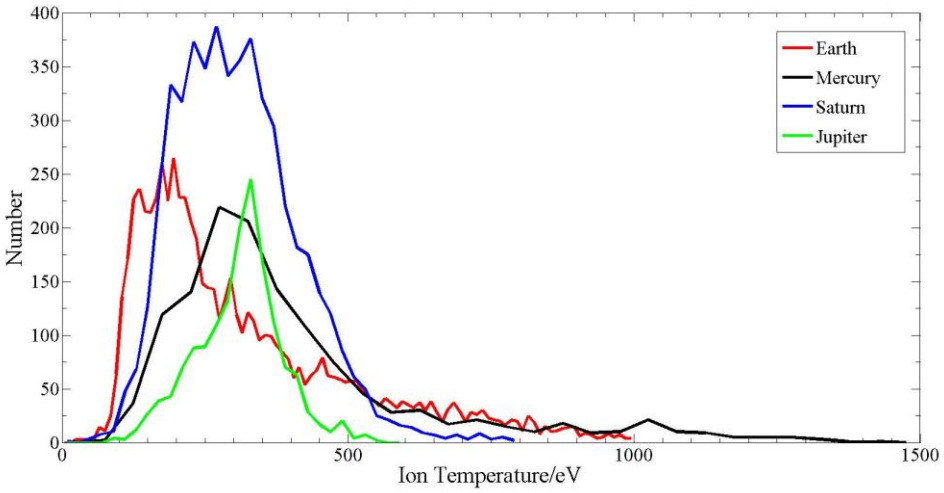

Figure. 3 Distributions of ion temperatures in the magnetosheaths of Mercury, Earth, Jupiter and Saturn.

As for Earth, we choose the data of the MMS1 satellite during the period from 2015 to 2016 for analysis. Examining the data during this period, we can find that there are 141 days when the detector was in the subsolar region (with the zenith angles from X axis being $<30^{\circ}$) of Earth's magnetosheath. Using the data within this interval, the distributions of ion temperatures and electron temperatures in Earth's magnetosheath can be obtained. The ion temperatures are derived from the ion vertical temperature $T_{i\perp}$ and the ion parallel temperature $T_{i||}$ in FPI_FAST_L2_DIS-MOMS of MMS1 and the electron temperatures are gained from the electron vertical temperature $T_{e\perp}$ and the electron parallel temperature $T_{e||}$ in FPI_FAST_L2_DES-MOMS of MMS1 with the data time resolution of 4.5s. The calculation formulas are $T_i = \frac{1}{3}T_{i||} + \frac{2}{3}T_{i\perp}$ and $T_e = \frac{1}{3}T_{e||} + \frac{2}{3}T_{e\perp}$. In the analysis of this article, we take a data point every 10 minutes. Figure 3 shows the distribution of ion temperatures in Earth's magnetosheath. It can be seen from the Figure 3 that, the

maximum ion temperature in Earth's magnetosheath can reach up to 1000eV, the average ion temperature is $\overline{T_i} \approx 319eV$, and the most probable value of ion temperature in Earth's magnetosheath is $T_{im} \approx 195eV$. The distribution of electron temperatures in Earth's magnetosheath is shown in Figure 4. It can be seen from the Figure that the maximum electron temperature can reach 120eV, the average electron temperature is $\overline{T_e} \approx 46eV$, and the most probable value of electron temperature is $T_{em} \approx 35eV$.

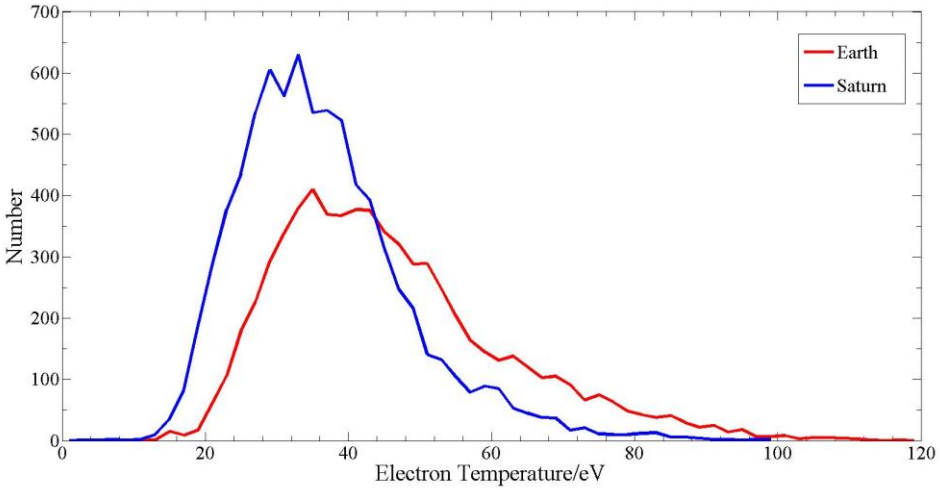

Figure. 4 Distributions of electron temperatures in the magnetosheaths of Earth and Saturn, which are obtained from the MMS1 and Cassini measurements, respectively.

Regarding Jupiter, we use the data of Voyager 2 satellite from July 2 to July 5, 1979. Proton temperatures used the ION-L-MODE data in PLS with the data time resolution of 96 s. The distribution of proton temperatures in Jupiter's magnetosheath is illustrated in Figure 3. It can be seen from Figure 3 that the maximum proton temperature in Jupiter's magnetosheath can reach 600eV, average proton temperature in Jupiter's magnetosheath is $\overline{T_P} \approx 310eV$, and the most probable value of the proton

temperature is $\overline{T}_{pm} \approx 330eV$.

For Saturn, we use the data of the Cassini satellite from 2007 to 2008. Counting the data from 2007 to 2008, we found that there are 66 days that the detector was located in the subsolar region (with the zenith angles from X axis being $<30^{\circ}$) of Saturn's magnetosheath. With the data during these 66 days periods, the distribution of plasmas temperatures in Saturn's magnetosheath can be obtained. Proton temperatures are derived from the DDR-ION-MOMENTS data in CAPS (Cassini Plasma Spectrometer) with the time resolution of ~ 7 minutes and electron temperatures are derived from the DDR-ELE-MOMENTS data in CAPS with the time resolution of ~ 32s. In the statistics of this paper, proton temperatures take one data point every 7 minutes, and electron temperatures take one data point every 5 minutes. Figure 3 presents the distribution of proton temperatures in Saturn's magnetosheath. It is shown in Figure 3 that the proton temperature can reach 800eV, the average proton temperature is $\overline{T_p} \approx 307eV$, and the most likely value of proton temperature is $T_{pm} \approx 270eV$. The distribution of electron temperatures in the magnetosheath of Saturn is presented in Figure 4, which indicates that, the electron temperature can reach 100eV, the average value of electron temperature is $\overline{T_e} \approx 36eV$, and its most measurable value is $T_{em} \approx 33eV$. Table 1 lists the relevant parameters of ion and electron temperatures in the magnetosheaths of Mercury, Earth, Jupiter and Saturn. We still can not find the electron observation data for the magnetosheaths of Mercury and Jupiter. The average plasma temperature of Earth's magnetosheath is $\langle T \rangle_{sh} \approx \frac{1}{2}\left(\overline{T}_e + \overline{T}_i\right) \approx 183eV \approx 2.12\text{MK}$ and 172eV, and 2.00MK, respectively, which

are very near to the average temperature of the solar corona. As for Suturn's magnetosheath, its average plasma temperature is $\langle T \rangle_{sh} \approx \frac{1}{2}\left(\bar{T}_e + \bar{T}_i\right) \approx 172eV \approx 2.00\text{MK}$, which is again about the average temperature of the solar corona. These statistical results confirm the theoretical results presented in the last Section. It can also be seen that, for both Earth's and Suturn's magnetosheaths, the electron temperatures are much less than the proton temperatures. The proton-electron temperature ratio in the magnetosheath of Earth and Suturn are 6.9 and 8.5, respectively. It is indicated that, as the solar wind are running out from the solar corona, the electrons have been cooled sufficiently.

Table 1

Ion and electron temperatures of the magnetosheaths as deduced from Mercury, Earth, Jupiter and Saturn observations.

Parameters / Planets	T_{pm}（eV）	$\overline{T_p}$（eV）	T_{em}（eV）	$\overline{T_e}$（eV）	$\langle T \rangle$（eV）	$\overline{T_p}/\overline{T_e}$
Mercury	275	414				
Earth	195	319	35	46	183	6.9
Jupiter	330	310				
Saturn	270	307	33	36	172	8.5

4 Discussion and Conclusions

The magnetosheaths supply matter and energy to planetary magnetospheres and play critical roles during the evolutions of the magnetospheres (Axfordet et al., 1961; Dungey, 1961; Phan et al., 2000; Fujimoto et al., 2008; Wang et al., 2012). The upstream solar wind plasmas, which originate from the solar corona, are compressed by the bow shocks so as to form the downstream magnetosheath plasmas. Obviously, the thermal properties of the planetary magnetosheaths are determined by the features of the solar corona. A lot of observational investigations have indicated that the temperatures of planetary magnetosheaths at the subsolar points are about several hundred eV or several MK (Gershman et al., 2013; Slavinet et al.,2014; Shen et al., 2008; Wang et al., 2012; Richardson, 1987, 2002; Sergiset et al., 2013), that are very close to the maximum temperature of the solar corona (Laming et al., 1995; Delaboudinière et al., 1995; Tu et al., 1999; Schrijveret et al.,1999; Schmelz et al., 2015). This research seeks to find the quantitative relationship between the temperatures of the solar corona and planetary magnetosheaths.

It is noted that the thermal energy of the solar corona that was converted into kinetic energy to accelerate the solar wind is almost entirely converted back to thermal energy when the plasma crosses the planetary bow shock. As viewed from the second law of thermodynamics, generally, the maximum temperatures of the planetary magnetosheaths cannot be higher than that of the solar corona. In this investigation, a detailed theoretical exploration has been made on the steady expansion of solar corona, the propagations of the solar wind and the compressions of planetary

magnetosheaths by the bow shocks. The method used is universal and fit for the dynamics of multiple components, thermal anisotropy and non-Maxwellian plasmas in a steady state. In the core region of the solar corona, the heating input and the radiative loss reach a thermal equilibrium, so as to maintain the extremely high temperature of the corona plasmas. At present, we still have not had a clear understanding on the real heating mechanism of the solar corona (McComas et al., 2007; Parnell et al., 2012; Klimchuk, 2015; Cranmer et al., 2017). In this research, we only study the outward expansion of the outer corona under the thermodynamic driving, evading the possible heating and radiation loss. This approximation is reasonable and will not seriously affect the results obtained in the work.

The formula for the relationship between the temperatures of the solar corona and planetary magnetosheaths has been approximately yielded. The quantitative results indicate that the maximum temperatures of all the planetary magnetosheaths at the subsolar points in the solar system have comparable values. In general, the maximum temperatures of the planetary magnetosheaths are lower than that of the solar corona. These theoretical results are consistent with the measurements on planetary magnetosheaths (Gershman et al., 2013; Slavinet et al., 2014; Shen et al., 2008; Wang et al., 2012; Richardson, 1987, 2002; Sergiset et al., 2013).

A systematic statistical investigation on the average temperatures of the magnetosheaths of Mercury, Earth, Jupiter and Suturn has been performed. It has been found that, the average proton temperatures of the magnetosheaths of Mercury, Earth, Jupiter and Suturn are 414eV, 319eV, 310eV and 307eV, respectively; while the

562 average electron temperatures of the magnetosheaths of Earth and Suturn are 46eV
563 and 36eV, respectively (no electron data for Mercury and Jupiter are available at
564 present). The average plasma temperatures of the magnetosheaths of Earth and Suturn
565 are 183eV and 172eV, respectively, or 2.12MK and 2.00MK, respectively, which are
566 about the average temperature of the solar corona. The statistical results are in
567 agreement with the theoretical results. However, the electrons have been cooled
568 considerably during the outward propagating of the solar wind.

569 The relationship between the temperatures of the solar corona and planetary
570 magnetosheaths obtained here can be applied to the steady corona, solar wind and
571 planetary magnetosheaths. These results can also be fit for the magnetosheaths of
572 Venus and Mars without intrinsic magnetic field (Øieroset et al., 2004). The
573 heliosheath is at the temperature of ~2MK as shown by the observations (Liu et al.,
574 2007), which can also be explained by the theoretical results in Section 2. It is shown
575 that the planetary magnetosheaths, ICME sheaths, and the heliosheath have similarity
576 in respect of hot protons (Richardson and Liu, 2007). These should also be applicable
577 for the steady fast solar wind originating from the coronal holes. However, the results
578 obtained in this investigation are not suitable for the explosive processes of the CMEs,
579 during which the coronal magnetic energy contributes to the outward acceleration of
580 the solar wind.

581 The relationship between the temperatures of the solar corona and planetary
582 magnetosheaths obtained here is useful for the evaluation on the thermal features of
583 the planetary magnetospheres based on the solar coronal conditions. The plasmas in

584 the tail plasma sheet are mainly originated from the magnetosheath. It is found that
585 the temperature ratio of protons and electrons in the Earth's plasma sheet is ~7, which
586 is about the same as that in the magnetosheath. The higher the temperature of the
587 magnetosheath, the higher that of the plasma sheet.

588

589

590 **Acknowledgments**

591 This work was supported by the National Natural Science Foundation of China Grant
592 No. 41874190 and 41231066. The authors are thankful to the Energetic Particle and
593 Plasma Spectrometer (EPPS) team and Magnetometer (MAG) team for providing
594 Messenger data (https://pds-ppi.igpp.ucla.edu), Plasma Subsystem (PLS) team and
595 MAG PI team for providing Voyager 2 data (https://pds-ppi.igpp.ucla.edu), Cassini
596 Plasma Spectrometer (CAPS) team for providing Cassini data
597 (https://pds-ppi.igpp.ucla.edu), and MMS team for providing the MMS data
598 (https://cdaweb.gsfc.nasa.gov). The authors thank Yu Liu, Zhaojin Rong, and Gang
599 Zeng for their help during preparing the manuscript.

600

601 **References**

602 Axford, W. I., & Hines, C. O. (1961). A unifying theory of high-latitude geophysical phenomena
603 and geomagnetic storms. Canadian Journal of Physics, 39(10), 1433-1464, doi:

10.1029/GM018p0936.

Barnes, & Aaron. (1992). Acceleration of the solar wind. Reviews of Geophysics, 30(1), 43, doi: 10.1029/91RG02816.

Burlaga, L. F., & Szabo, A. . (1999). Fast and slow flows in the solar wind near the ecliptic at 1 au?. Space Science Reviews, 87(1-2), 137-140, doi: 10.1023/A:1005186720589.

Chao, J. K., D. J. Wu, C.-H. Lin, Y. H. Yang, and X. Y. Wang (2002), Models for the size and shape of the Earth's magnetopause and bow shock, in *Space Weather Study Using Multipoint Techniques*, edited by L.-H. Lyu, 360 pp., Pergamon, New York.

Chapman, S., and V. C. A. Ferraro (1930), A new theory of magnetic storms, Nature, 126, 129–130, doi: 10.1029/TE036i003p00171.

Chapman, J. F., I. H. Cairns, J. G. Lyon, and C. R. Boshuizen (2004), MHD simulations of Earth's bow shock: Interplanetary magnetic field orientation effects on shape and position, J. Geophys. Res., 109, A04215, doi:10.1029/2003JA010235.

Christon, S. P., D. G. Mitchell, D. J. Williams, L. A. Frank, C. Y. Huang, and T. E. Eastman (1988), Energy spectra of plasma sheet ions and electrons from about 50 eV/e to about 1 MeV during plasma temperature transitions, *J. Geophys. Res.*, *93*, 2562–2572, doi:10.1029/JA093iA04p02562.

Cranmer, S. R., S. E. Gibson, and P. Riley (2017), Origins of the ambient solar wind: implications for space weather, Space Science Reviews, 212, 1-40, doi: 10.1007/s11214-017-0416-y.

Cranmer, S. R., W. H. Matthaeus, B. A. Breech, and J. C. Kasper(2009), Empirical Constraints on Proton and Electron Heating in the Fast Solar Wind, Astrophysical Journal, 702, 1604-1614, doi:

625 10.1088/0004-637X/702/2/1604.

626 De Moortel, I., and P. Browning (2015), Recent advances in coronal heating, Phil. Trans. R. Soc. A
627 373, 20140269, doi: 10.1098/rsta.2014.0269.

628 Delaboudinière, J.-P. et al. (1995), EIT: Extreme-ultraviolet Imaging Telescope for the SOHO
629 mission,Solar Phys. 162, 291, doi: 10.1007/BF00733432.

630 Dmitriev, A. V., J. K. Chao, and D.-J. Wu (2003), Comparative study of bow shock models using
631 Wind and Geotail observations, J. Geophys. Res., 108, 1464, doi:10.1029/2003JA010027.

632 Dungey, J. W. (1961), Interplanetary magnetic field and the auroral zones, Phys. Rev. Lett., 6,
633 47–48, doi: 10.1103/PhysRevLett. 6. 47.

634 Echim, M. M., J. Lemaire, and Øystein Lie-Svendsen (2011), A review on solar wind modeling:
635 kinetic and fluid aspects, Surveys in Geophysics, 32, 1-70, doi: 10.1007/s10712-010-9106-y.

636 Feldman W. C., Asbridge J. R., Bame S. J., Montgomery M. D., Gary S. P., 1975, J.
637 Geophys. Res., 80, 4181

638 Feldman W. C., R. C. Anderson, S. J. Bame, S. P. Gary, J. T. Gosling, D. J. McComas,
639 M. F. Thomsen, G. Paschmann, and M. M. Hoppe (1983a), J. Geophys. Res., 88, 96

640 Feldman W. C., R. C. Anderson, S. J. Bame, J. T. Gosling, R. D. Zwickl, and E. J.
641 Smith (1983b), J. Geophys. Res., 88, 9949-9958.

642 Fujimoto, M., T., T. Terasawa, Y. Mukai, T. Saito, et al. (1998), Plasma entry from the flanks of the
643 near-Earth magnetotail: Geotail observations, J., Geophys. Res., 103, 4391-4408, doi:
644 10.1029/97JA03340.

645 Gaelzer R., Ziebell L. F., Vi˜nas A. F., Yoon P. H., Ryu C. M., 2008, Asymmetric solar
646 wind electron superthermal distributions, Astrophysical J., 677, 676-682.

647 Gershman, D. J., J. A. Slavin, , J. M. Raines, et al. (2013), Magnetic flux pileup and plasma
648 depletion in Mercury's subsolar magnetosheath, J. Geophys. Res. Space Physics, 118,
649 7181–7199, doi: 10.1002/2013JA019244.

650 Hudson, P. D. (1970), Discontinuities in an anisotropic plasma and their identification in the solar
651 wind, Planet. Space Sci., 18, 1611–1622, doi: 10.1016/0032-0633(70)90036-X.

652 Klimchuk, J. A. (2015), Key aspects of coronal heating. Phil. Trans. R. Soc. A, 373, 20140256, doi:
653 10.1098/rsta.2014.0256.

654 Ko, Y.-K., and C. P. T. Groth (1999), Electron temperature and heating in the fast solar wind,
655 Space Science Reviews, 87, 227–231.

656 Laming, J. M., J. J. Drake, and K. G. Widing (1995), Stellar coronal abundances. 3: The solar first
657 ionization potential effect determined from full-disk observation, Astrophys. J. 443, L416, doi:
658 10.1086/175534.

659 Lin R.P. (1998), WIND observations of superthermal electrons in the interplanetary
660 medium, Space Sci. Rev., 86, 61-78.

661 Liu, Y., et al. (2007), Temperature Anisotropy in a Shocked Plasma: Mirror-Mode Instabilities in
662 the Heliosheath, Astrophysical Journal, 659, 391, doi: 10.1086/516568.

663 Liu, Z.-X., C. P. Escoubet, Z. Pu, et al. (2005), The Double Star Mission, Ann Geophysicae, 23,
664 2707-2712, doi: 10.5194/angeo-23-2707-2005.

665 Maksimovic, Milan, V. Pierrard, and P. Riley (1997), Ulysses electron distributions fitted with
666 Kappa functions. Geophysical Research Letters, 24,1151-0, doi: 10.1029/97GL00992.

667 Marsch, E. (1999). Solar wind models from the sun to 1 au: constraints by in situ and remote
668 sensing measurements. Space Science Reviews, 87(1-2), 1-24, doi: 10.1023/A:1005137311503.

669 Marsch E. (2006), Kinetic physics of the solar corona and solar wind, Living Rev.
670 Solar Phys., 3, 1. https://doi.org/10.12942/lrsp-2006-1

671 Masood, W., S. J. Schwartz, M. Maksimovic, A. N. Fazakerley (2006), Ann. Geophys., 24, 1725.

672 Masters, A., S. J. Schwartz, E. M. Henley, M. F. Thomsen, B. Zieger, A. J. Coates, N. Achilleos, J.
673 Mitchell, K. C.Hansen, and M. K. Dougherty (2011), Electron heating at Saturn's bow shock, J.
674 Geophys. Res., 116, A10107, doi:10.1029/2011JA016941.

675 McComas, D. J., et al. (2007), Understanding coronal heating and solar wind acceleration: Case
676 for in situ near-Sun measurements, Rev. Geophys., 45, RG1004, doi: 10.1029/2006RG000195.

677 McComas, D. J., Ebert, R. W., Elliott, H. A., Goldstein, B. E., Gosling, J. T., Schwadron, N. A., &
678 Skoug, R. M. (2008). Weaker solar wind from the polar coronal holes and the whole Sun.
679 Geophysical Research Letters, 35(18), doi: 10.1029/2008GL034896.

680 Øieroset, M. et al. (2004), The Magnetic Field Pile-up and Density Depletion in the
681 MartianMagnetosheath: A Comparison with the Plasma Depletion Layer Upstream of the
682 Earth's Magnetopause, Space Science Reviews, 111,185–202,
683 doi:10.1023/B:SPAC.0000032715.69695.9c.

684 Parker, E. N. (1958), Dynamics of the interplanetary gas and magnetic fields, Astrophys. J., 128,
685 644, doi: 10.1086/146579.

686 Parnell, C. E., & De Moortel, I. (2012). A contemporary view of coronal heating. Philosophical
687 Transactions of the Royal Society A: Mathematical, Physical and Engineering Sciences,
688 370(1970), 3217-3240, doi: 10.1098/rsta.2012.0113.

689 Petrinec, S. M., and C. T. Russell (1997), Hydrodynamic and mhd equations across the bow shock
690 and along the surfaces of planetary obstacles, Space Science Reviews, 79, 757-791, doi:
691 10.1023/A:1004938724300.

692 Phan, T. D., Lin, R. P., Fuselier, S. A., & Fujimoto, M. (2000), Wind observations of mixed
693 magnetosheath-plasma sheet ions deep inside the magnetosphere. Journal of Geophysical
694 Research Space Physics,105(A3), 5497-5505, doi: 10.1029/1999JA900455.

695 Pierrard, V., and J. Lemaire (1996), Lorentzian ion exosphere model, *J. Geophys. Res.*,
696 *101*, 7923–7934.

697 Pierrard, V., H. Lamy, and J. F. Lemaire (2004), Exospheric distributions of minor
698 ions in the solar wind, *J. Geophys. Res.*, *109*, A02118,
699 doi:10.1029/2003JA010069.Qureshi, M. N. S., Nasir, W., Masood, W., Yoon, P. H., &
700 Schwartz, S. J. . (2014). Terrestrial lion roars and non-maxwellian distribution. Journal of
701 Geophysical Research: Space Physics, 119(12), 10,059-10,067, doi: 10.1002/2014JA020476.

702 Qureshi M. N. S., Shah H. A., Murtaza G., Schwartz S. J., Mahmood F., 2004, Parallel
703 propagating electromagnetic modes with the generalized (r,q) distribution function,
704 Phys. Plasmas, 11, 3819-3829.

705 Qureshi M. N. S., Warda Nasir, Bruno, R., Masood, W., 2019, Whistler instability
706 based on observed flat-top two-component electron distributions in the Earth's

magnetosphere, MNRAS, 488, 954-964.

Richardson, J. D. (2002), The magnetosheaths of the outer planets, Planetary and Space Science, 50, 503 – 517, doi: 10.1016/S0032-0633(02)00029-6.

Richardson, J.D. (1987), Ion distribution functions in the dayside magnetosheaths of Jupiter and Saturn, J. Geophys. Res. 92, 6133, doi: 10.1029/JA092iA06p06133.

Rossi, B., and S. Olbert (1970), Introduction to the Physics of Space, (New York: Mcgraw-Hill Book Company), 298.

Schippers, P., et al. (2008), Multi-instrument analysis of electron populations in Saturn's magnetosphere, *J. Geophys. Res.*, *113*, A07208, doi:10.1029/2008JA013098.

Schmelz, J. T., & Winebarger, A. R. (2015). What can observations tell us about coronal heating?. Philosophical Transactions of the Royal Society A: Mathematical, Physical and Engineering Sciences, 373(2042), 20140257, doi: 10.1098/rsta.2014.0257.

Schrijver, C. J., Berger, T. E., Fletcher, L., Hurlburt, N. E., Nightingale, R. W., Shine, R. A., ... & Deluca, E. E. (1999). A new view of the solar outer atmosphere by the Transition Region and Coronal Explorer. Solar Physics, 187(2), 261-302, doi: 10.1023/A:1005194519642.

Sckopke, N., Paschmann, G., Brinca, A. L., Carlson, C. W., and H. Lühr (1990), Ion thermalization in quasi-perpendicular shocks involving reflected ions, Journal of Geophysical Research Space Physics, 95.

Scudder, J. D. (2015), Radial variation of the solar wind proton temperature: heat flow or addition? Astrophysical Journal,809, 126, doi: 10.1088/0004-637X/809/2/126.

728 Sehar Sumbul, Qureshi, M. N. S., Shah, H. A., 2019, Electron acoustic instability in
729 four component space plasmas with observed generalized (r,q) distribution function,
730 AIP Advances, 9, 025315.

731 Sergis, N., C. M. Jackman, A. Masters, S. M. Krimigis, et al. (2013), Particle and magnetic field
732 properties of the Saturnian magnetosheath: presence and upstream escape of hot
733 magnetospheric plasma, J. Geophys. Res. Space Physics, 118, 1620–1634, doi:
734 10.1002/jgra.50164.

735 Shen, C., and Z. -X. Liu (2005), Double Star Project Master Science Operations Plan, Ann.
736 Geophysicae, 23, 2851-2859, doi: 10.5194/angeo-23-2851-2005.

737 Shen, C. et al. (2008), Surveys on Magnetospheric Plasmas Based by DSP exploration, Sci. in
738 China, 51, 1639-1647, DOI: 10.1007/s11431-008-0252-0.

739 Shen, C., M. Dunlop, X. Li, Z. X. Liu, A. Balogh, T. L. Zhang, C. M. Carr, Q. Q. Shi, and Z. Q.
740 Chen (2007), New approach for determining the normal of the bow shock based on Cluster
741 four-point magnetic field measurements, J. Geophys. Res., 112, A03201,
742 doi:10.1029/2006JA011699.

743 Shen, C., Zeng, G., Zhang, C., Rong, Z., Dunlop, M., Russell, C. T., et al. (2020). Determination
744 of the configurations of boundaries in space. Journal of Geophysical Research: Space Physics,
745 125, e2020JA028163. https://doi.org/10.1029/2020JA028163

746 Shue, J.-H., et al. (1998), Magnetopause location under extreme solar wind conditions, J. Geophys.
747 Res., 103, 17,691–17,700,doi:10.1029/98JA01103.

748 Slavin, J. A., et al. (2014), MESSENGER observations of Mercury's dayside magnetosphere under

749 extreme solar wind conditions, J. Geophys. Res. Space Physics, 119,
750 doi:10.1002/2014JA020319.

751 Song, P., C. T. Russell, J. T. Gosling, M. F. Thomsen, and R. C. Elphic (1990), Observations of the
752 density profile in the magnetosheath near the stagnation streamline, Geophys. Res. Lett., 17,
753 2,035.

754 Song, P., C. T. Russell, and M. F. Thomsen (1992), Slow mode transition in the
755 frontside magnetosheath. *Journal of Geophysical Research Space Physics*, *97*(A6),
756 8295-8305.

757 Song, P., C. T. Russell, and S. P. Gary (1994), Identification of low-frequency
758 fluctuations in the terrestrial magnetosheath, J. Geophys. Res., 99, 6011.

759 Song, P. , Russell, C. T. , Gombosi, T. I. , Spreiter, J. R. , Stahara, S. S. , & Zhang, X.
760 X. . (1999a), On the processes in the terrestrial magnetosheath 1. scheme
761 development. *Journal of Geophysical Research Space Physics*, *104*(A10),
762 22345-22355.

763 Song, P. , Russell, C. T. , Zhang, X. X. , Stahara, S. S. , Spreiter, J. R. , & Gombosi, T.
764 I. . (1999b), On the processes in the terrestrial magnetosheath 2. case study. *Journal*
765 *of Geophysical Research: Space Physics*, *104*(A10), 22357.

766 Spreiter, J. R., and A. Y. Alksne (1969), Plasma flow around the magnetosphere, Rev.
767 Geophys., 7, 11.

768 Southwood, D. J. , & Kivelson, M. G. . (2020). An improbable collaboration. *Journal*
769 *of Geophysical Research: Space Physics*, in submission.

770 Southwood, D. J., & Kivelson, M. G. (1995), The formation of slow mode fronts in

771 the magnetosheath, p. 109 in AGU Monograph 90, Physics of Magnetopause,
772 edited by P. Song & B.U.O. Sonnerup, AGU, Washington, D.C.

773 Thomsen M. F., Coates A. J., Jackman C. M., et al. (2018), Survey of magnetosheath plasma
774 properties at Saturn and inference of upstream flow conditions, Journal of Geophysical
775 Research: Space Physics, 123, 2034, doi: 10.1002/2018JA025214.

776 Tu, C. Y. , E. Marsch, and K.Wilhelm (1999), Ion temperatures as observed in a solar coronal hole.
777 Space Science Reviews, 87(1), 331-334, doi: 10.1023/A:1005154030100.

778 Taylor, M. G. G. T., B. Lavraud, C. P. Escoubet, et al. (2008), The plasma sheet and boundary
779 layers under northward IMF: A multi-point and multi-instrument perspective, Advances in
780 Space Research, 41, 1619-1629, doi: 10.1016/j.asr.2007.10.013.

781 Vasyliunas, V. M. (1968), A crude estimate of the relation between the solar wind speed and the
782 magnetospheric electric field, J. Geophys. Res., 73, 2839, doi: 10.1029/JA073i007p02529.

783 Wang, C.-P., M. Gkioulidou, L. R. Lyons, and V. Angelopoulos (2012), Spatial distributions of the
784 ion to electron temperature ratio in the magnetosheath and plasma sheet, J. Geophys. Res., 117,
785 A08215, doi:10.1029/2012JA017658.

786 Weber, E. ~J , and L. Davis(1967), The angular momentum of the solar wind, Astrophysical
787 Journal , 148.3P1, 217-227.

788 Zwan, B. J., and R. A. Wolf (1976), Depletion of solar wind plasma near a planetary
789 boundary, *J. Geophys. Res., 81*.

790